

See discussions, stats, and author profiles for this publication at: <https://www.researchgate.net/publication/49846551>

# Effect of Solvation on Ion Binding to Imidazole and Methylimidazole

ARTICLE *in* THE JOURNAL OF PHYSICAL CHEMISTRY A · FEBRUARY 2011

Impact Factor: 2.69 · DOI: 10.1021/jp1120492 · Source: PubMed

---

CITATIONS

19

READS

33

## 3 AUTHORS, INCLUDING:



Bhaskar Sharma

Pierre and Marie Curie University - Paris 6

4 PUBLICATIONS 31 CITATIONS

[SEE PROFILE](#)



G Narahari Sastry

Indian Institute of Chemical Technology

262 PUBLICATIONS 5,279 CITATIONS

[SEE PROFILE](#)

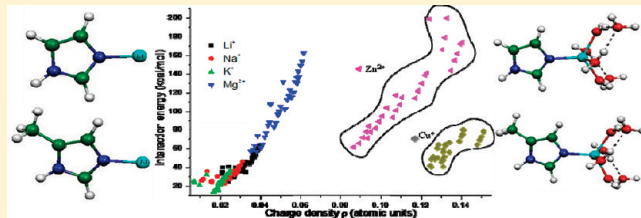
# Effect of Solvation on Ion Binding to Imidazole and Methylimidazole

Bhaskar Sharma, J. Srinivasa Rao, and G. Narahari Sastry\*

Molecular Modeling Group, Organic Chemical Sciences, Indian Institute of Chemical Technology, Tarnaka, Hyderabad 500 607, AP, India

S Supporting Information

**ABSTRACT:** Quantum chemical [MP2(FULL)/6-311++G(d,p)] calculations are done on the binding of hydrated  $\text{Li}^+$ ,  $\text{Na}^+$ ,  $\text{K}^+$ ,  $\text{Mg}^{2+}$ ,  $\text{Cu}^+$ , and  $\text{Zn}^{2+}$  metal ions with biologically relevant heteroaromatics such as imidazole and methylimidazole. The computed interaction energies are found to be in good agreement with the available experimental data. The effect of hydration on hydrogen bonding has been studied in detail and it shows that the hydrogen bond strength between  $\text{H}_2\text{O}\cdots\text{H}-\text{N}(1)$  substantially increases in the presence of metal ions. The present study quantifies the cooperativity between  $\text{M}\cdots\cdots\text{imidazole}$  ( $\text{M} = \text{Li}^+, \text{Na}^+, \text{K}^+, \text{Mg}^{2+}, \text{Cu}^+$ , and  $\text{Zn}^{2+}$ ) and  $\text{N}(1)-\text{H}\cdots\cdots\text{OH}_2$  interactions. Topological atoms in molecules (AIM) analysis and charge analysis support the variation in hydrogen-bonding strength and the variation in  $\text{M}\cdots\cdots\text{imidazole}$  binding strength. Effect of hydration on  $\text{N}(1)-\text{H}$  stretching frequency is studied, and it shows a clear shift in the stretching frequency after sequential hydration of metal ion as well as the  $\text{N}(1)$  of imidazole. The present study provides a detailed account on the biologically important  $\text{M}-\text{histidine}$  motif interaction with metal ions, where histidine is modeled by imidazole and methylimidazole.



## INTRODUCTION

Metal ions have a profound influence on the structure, stability, and reactivity of biomolecules and often play a triggering role in their functions. The interaction of metal ions with aromatic amino acids is of fundamental interest, as it found to stabilize the  $\pi-\pi$  stacking interactions and also trigger a fruitful interplay between theory and experiment.<sup>1–4</sup> The two most prominent naturally occurring heterocyclic motifs, namely imidazole and methylimidazole in histidine side chains, bind with metal ion in  $\sigma$  fashion.<sup>5</sup> There was considerable interest in probing the metal ion interaction with imidazole, because the gas-phase zwitterionic forms of amino acids are stabilized by divalent metal ions.<sup>6</sup> It has been found that the partial or full hydration of zwitterions results not only in their stabilization but also effects the functions of biomolecules.<sup>8,9</sup> Our earlier studies have established that metal ion complexation and explicitly accounting for the hydration effect are of high significance in probing the nature and elucidation of the structure of macromolecules.<sup>10</sup> It has been demonstrated that the solvation has a dramatic effect on the cation– $\pi$  interactions with selective solvation of one of the faces of metal ion and  $\pi$  system leading to seemingly contrasting effects.<sup>10</sup> Metal ion interactions with aromatic motifs have been extensively studied and their occurrence in proteins has been carefully analyzed and made available in the form of a database.<sup>11</sup> Among the aromatic motifs, histidine is one of the most frequently occurring residues in the metal binding regions.<sup>12</sup> Several crystallographic studies have been done to understand the functions of metal ions in the active site,<sup>13</sup> and histidine is one of the most ubiquitous residue in the metal binding sites. For the most part, it has been found in the case of histidine that the preferential

approach of metal ion is along the molecular plane of the imidazole ring through its N center.<sup>12a</sup>

In recent years, many computational and experimental studies reported the energetic and the conformational changes of aromatic amines, amino acids, and small peptides, when they bind to mono- and divalent metal ions in the presence and absence of explicit solvent.<sup>14</sup> Binding of mono- and divalent metal ions (both in bare and hydrated forms) with nucleic acids was extensively studied by Leszczynski and co-workers.<sup>15</sup> Earlier, experimental and theoretical studies directed to probe the metal ion interaction with imidazole have been reported.<sup>16</sup> Hydration of neutral and cationic imidazole is done by means of ab initio, molecular dynamics, and photoelectron spectroscopy. From the earlier literature it is clear that, for ionization of neutral imidazole, the long-range polarization of the water solvent by the solute needs to be considered.<sup>17,18</sup> Earlier studies were aimed at the study of metal ion base pair complexes in nucleic acids, and hydration has been implicated to switch preferences for stacking of it in the presence of cations such as  $\text{Mg}^{2+}$ .<sup>19</sup> Thus, hydration is expected to play an important role in not only the structure and energetics of metal ion complexes in biomolecules but also how it effects in the neighboring supramolecular interactions.

The objective of the current study is to understand the variations of hydrogen-bonding ability in imidazole and methylimidazole complexes upon the metal ion complexation. The methylimidazole is chosen to mimic the side chain residue of

Received: September 3, 2010

Revised: January 25, 2011

Published: February 21, 2011

histidine. One key feature of the noncovalent interactions is that a large number of them operate simultaneously and their complexation energies are often nonadditive. In the case of metal ion interaction with aromatic motifs, we have demonstrated that the size of the  $\pi$ -acceptor has dramatic effect on the complexation energies.<sup>20</sup> The other important feature is the way in which two noncovalent interactions influence each other. In the earlier studies, it has been computationally demonstrated that cation– $\pi$  interactions engage themselves in highly cooperative fashion with neighboring hydrogen-bonding and stacking interactions.<sup>21</sup> The cooperativity thus manifested between a pair of noncovalent interactions has been quantified in earlier cases.<sup>21</sup> While studying the solvation of metal ion is interesting in its own right, replacing one or more coordination sites with the biologically important motifs imidazole and methylimidazole is of relevance, considering their resemblance to the metal binding site in biomacromolecules.

In the current study, as is shown in Scheme 1, we have taken imidazole and methylimidazole complexed with metal ( $M = Li^+, Na^+, K^+, Mg^{2+}, Cu^+$ , and  $Zn^{2+}$ ) ions as model systems and study the effect of explicit solvent (water) using high level ab initio and DFT methodologies. The bonding of alkali and alkaline earth metal ions is weaker, compared to those involving transition metals with the  $\pi$ -system and the lone pair bearing centers. The central transition metal ions such as  $Fe^{2+}$ ,  $Fe^{3+}$ , and  $Co^{2+}$  have bonding patterns with the  $\pi$ -system that are in high contrast to nonbonded interactions. However, the late transition metal ions considered in the study,

### Scheme 1

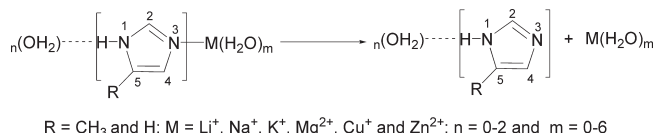


**Table 1. BSSE-Corrected Interaction Energies ( $\Delta E_{AB-C}$  in kcal/mol) of All Imi–M Complexes Calculated at Various Levels of Theory**

complex	M = $Li^+$		M = $Na^+$		M = $K^+$		M = $Mg^{2+}$		M = $Cu^+$		M = $Zn^{2+}$	
	MP2 <sup>a</sup>	B3LYP <sup>b</sup>	MP2 <sup>a</sup>	B3LYP <sup>b</sup>	MP2 <sup>a</sup>	B3LYP <sup>b</sup>	MP2 <sup>a</sup>	B3LYP <sup>b</sup>	MP2 <sup>a</sup>	B3LYP <sup>b</sup>	MP2 <sup>a</sup>	B3LYP <sup>b</sup>
Imi-0W	50.63 (50.4) <sup>c</sup>	53.28	35.51 (33.3) <sup>c</sup>	38.03	27.09 (26.1) <sup>c</sup>	27.50	130.25	139.12	64.30	70.91	166.15	185.75
Imi-1Wa	43.35	45.08	31.53	33.38	23.80	23.80	115.22	121.22	67.82	68.72	143.68	155.63
Imi-1Wb	57.87	60.69	41.61	44.31	32.39	32.90	149.10 <sup>d</sup>	158.78 <sup>d</sup>	72.62 <sup>d</sup>	79.76 <sup>d</sup>	187.92	210.14
Imi-1Wc	34.63	36.52	26.44	27.87	21.11	23.13						
Imi-2Wa	35.86	36.94	27.12	28.12	20.94	20.64	131.68	101.29	50.09	51.69	114.38	120.98
Imi-2Wb	49.70	51.55	37.02	39.03	28.60	28.70	131.68	138.17	75.08	77.16	161.95	175.19
Imi-2Wc	63.21	66.09	46.21	49.16	36.58	37.13	162.80	172.21	78.70	87.08	199.97	222.92
Imi-3Wa	29.32	28.19	22.89	22.84	18.00	17.10	83.24	84.34	41.68	42.04	93.31	96.47
Imi-3Wb	41.64	42.02	32.11	33.13	25.28	25.02	112.76	116.38	59.05	60.41	130.21	137.73
Imi-3Wc	54.42	56.31	41.22	43.29	32.39	32.50	142.84	149.58	80.35	82.63	173.72	187.43
Imi-4Wa	33.14	31.31	26.01	26.49	23.73	22.79	72.48	71.78	47.42	46.59	81.82	82.95
Imi-4Wb	35.07	34.13	27.52	27.52	22.44	22.28	96.53	98.33	48.40	48.94	107.43	111.27
Imi-4Wc	45.99	46.37	35.90	36.98	28.61	28.34	123.01	126.71	64.35	65.72	141.02	148.95
Imi-5Wa	29.34	27.79	25.82	24.77	19.80	19.79	59.17	56.78	47.59	46.04	65.85	64.93
Imi-5Wb	39.84	38.16	30.49	29.99	28.85	29.16	84.99	84.97	40.67	52.34	94.74	96.40
Imi-5Wc	39.95	38.86	34.99	35.93	32.06	31.19	105.93	124.64	66.45	65.79	117.46	121.67
Imi-6Wa	24.80	22.69	24.11	22.95	13.48	12.16	61.24	60.00	45.26	43.27	71.26	71.18
Imi-6Wb	34.30	30.04	32.36	32.62	−32.74	32.60	56.69	56.38	60.25	58.06	77.91	77.35
Imi-6Wc	<sup>f</sup>	<sup>f</sup>	<sup>f</sup>	<sup>f</sup>	<sup>f</sup>	<sup>f</sup>	107.87	105.63	57.40	56.20	104.14	106.15
Imi-6Wd	30.72	28.15	<sup>e</sup>	<sup>e</sup>	20.90	20.16	56.79	54.04	40.47	39.56	61.73	60.14

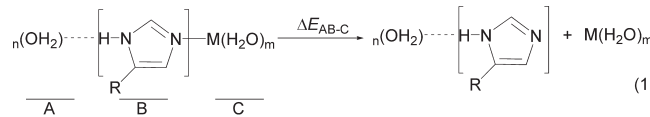
<sup>a</sup> MP2(FULL)/6-311++G(d,p)//B3LYP/6-31G(d,p). <sup>b</sup> B3LYP/6-311++G(d,p)//B3LYP/6-31G(d,p). <sup>c</sup> Values taken from ref 12a. <sup>d</sup> Leads to N(3) protonation of imidazole. <sup>e</sup> The corresponding  $Na^+$  complex could not be located on the potential energy surface. <sup>f</sup> The corresponding alkali metal complexes are not minima on the potential energy surface.

namely,  $Cu^+$  and  $Zn^{2+}$ , are comparable in their nature with alkali and alkali earth metal ions. Therefore, we included them in the study considering their biological relevance. The systematic study undertaken here aids in addressing the following points: (a) to gauge the influence of metal ion on hydrogen bonding between solvent molecules and imidazole, (b) to study the effect of solvation on cooperativity, and (c) to observe the changes in structural parameters upon solvation of metal ions as well as imidazole or methylimidazole.

### COMPUTATIONAL DETAILS

All complexes (Imi–M and Me-Imi–M; Imi = imidazole, Me-Imi = methylimidazole, M =  $Li^+, Na^+, K^+, Mg^{2+}, Cu^+$ , and  $Zn^{2+}$ ) are subjected to geometry optimization without imposing any symmetry constraints at the B3LYP/6-31G(d,p) level of theory. Frequency calculations are also performed at the same level to

### Scheme 2



$$R = CH_3 \text{ and } H; M = Li^+, Na^+, K^+, Mg^{2+}, Cu^+ \text{ and } Zn^{2+}; n = 0-2 \text{ and } m = 0-6$$

$\Delta E_{AB-C}$  = Interaction Energy

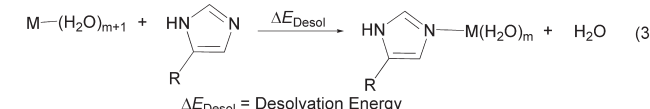
$$\Delta E_{coop} = \Delta_{ABC} - \Delta_{AB} - \Delta_{BC} - \Delta_{AC}$$

where  $\Delta_{ABC} = E_{ABC} - E_{AB} - E_C$  (2a)

$\Delta_{AB} = E_{AB} - E_A - E_B$  (2b)

$\Delta_{BC} = E_{BC} - E_B - E_C$  (2c)

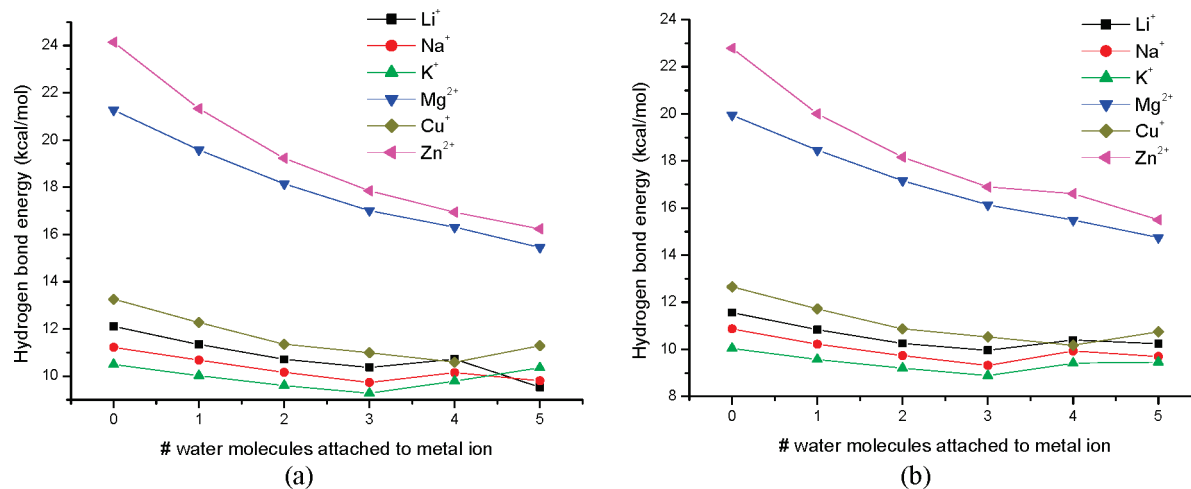
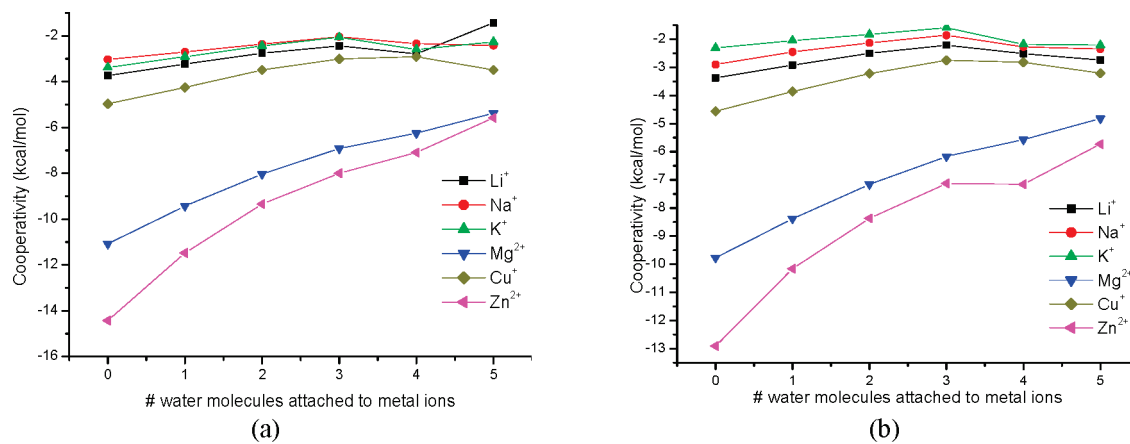
$\Delta_{AC} = E_{AC} - E_A - E_C$  (2d)



**Table 2.** BSSE-Corrected Interaction Energies ( $\Delta E_{AB-C}$  in kcal/mol) of All Me—Imi—M Complexes Calculated at Various Levels of Theory

complex	M = Li <sup>+</sup>		M = Na <sup>+</sup>		M = K <sup>+</sup>		M = Mg <sup>2+</sup>		M = Cu <sup>+</sup>		M = Zn <sup>2+</sup>	
	MP2 <sup>a</sup>	B3LYP <sup>b</sup>	MP2 <sup>a</sup>	B3LYP <sup>b</sup>	MP2 <sup>a</sup>	B3LYP <sup>b</sup>	MP2 <sup>a</sup>	B3LYP <sup>b</sup>	MP2 <sup>a</sup>	B3LYP <sup>b</sup>	MP2 <sup>a</sup>	B3LYP <sup>b</sup>
Me-Imi-0W	52.98	55.92	37.42	40.20	28.70	29.33	136.53	146.25	69.25	74.04	179.08	194.46
Me-Imi-1Wa	45.38	47.38	33.21	35.35	25.27	25.69	120.72	128.72	72.56	71.52	154.74	162.79
Me-Imi-1Wb	59.80	62.99	42.31	45.19	33.76	34.57	153.91	164.30	77.40	82.51	198.93	219.12
Me-Imi-2Wa	37.65	37.95	28.60	29.87	22.19	22.71	103.01	106.71	56.45	55.55	121.62	127.12
Me-Imi-2Wb	51.40	53.56	38.44	40.77	29.81	30.22	136.02	143.12	79.63	78.65	172.14	180.78
Me-Imi-3Wa	31.04	30.19	24.13	24.28	15.50	18.37	87.64	89.11	48.77	47.74	101.30	101.83
Me-Imi-3Wb	43.16	43.82	33.37	34.77	26.34	26.40	116.70	120.75	63.12	62.34	138.96	142.73
Me-Imi-4Wa	35.38	33.89	27.62	28.20	25.51	25.71	76.65	76.19	55.93	52.98	89.02	87.80
Me-Imi-4Wb	36.60	35.61	28.49	28.78	23.43	23.02	100.10	101.84	51.88	50.55	115.08	115.98
Me-Imi-5Wa	31.51	30.08	27.62	26.87	25.16	24.58	62.93	60.72	51.02	48.09	72.15	69.22
Me-Imi-5Wb	40.77	39.38	34.67	34.36	30.15	30.60	88.38	88.12	56.50	46.84	122.52	124.78
Me-Imi-6Wa	26.27	23.95	25.66	24.74	14.23	13.10	64.67	-63.15	48.63	45.28	77.74	75.74
Me-Imi-6Wb	36.96	37.39	35.75	35.32	32.04	31.96	73.78	-71.69	64.09	60.09	84.12	81.20

<sup>a</sup> MP2(FULL)/6-311++G(d,p)//B3LYP/6-31G(d,p). <sup>b</sup> B3LYP/6-311++G(d,p)//B3LYP/6-31G(d,p).

**Figure 1.** Variation in the strength of hydrogen bonding with the number of water molecules attached to metal ion in the (a) imidazole and (b) methylimidazole complexes.**Figure 2.** Correlation of cooperativity [MP2(FULL)/6-311++G(d,p)//B3LYP/6-31G(d,p)] with the number of water molecules in the (a) imidazole and (b) methylimidazole complexes.

ascertain the nature of stationary points on potential energy surface. The stationary points retrieved from several putative structures turned out to be transition structures or higher order saddle points. The direction of the imaginary frequencies was explored to obtain

the true minima on the potential energy surface. By taking the optimized geometries of the B3LYP/6-31G(d,p) level, single point energy calculations are performed at the MP2(FULL)/6-311++G(d,p) and B3LYP/6-311++G(d,p) levels of theory. Computed

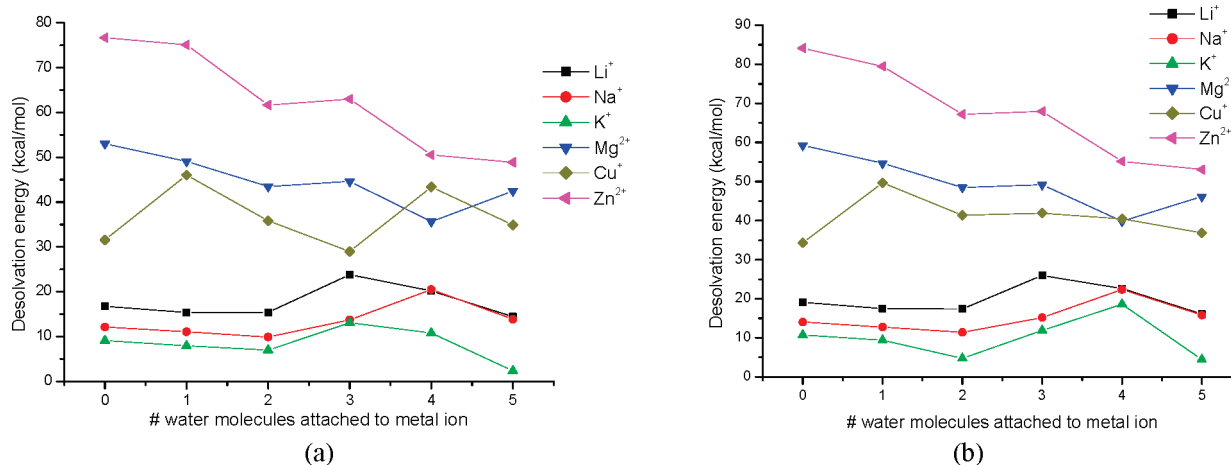


Figure 3. Variation in desolvation energy with the number of water molecules attached to the metal ion in the (a) imidazole and (b) methylimidazole complexes.

interaction energies are corrected for basis set superposition error (BSSE) by using the Boys–Bernardi counterpoise correction.<sup>22</sup> To understand the nature of metal–nitrogen interaction in the presence of solvent, the atoms in molecule (AIM) theory of Bader was applied.<sup>23</sup> AIM calculations were performed on geometries obtained at the B3LYP/6-31G(d,p) level. Interaction energies of metal ions with imidazole and methylimidazole are computed using Scheme 2. All calculations are performed using the Gaussian 03 suite of programs.<sup>24</sup>

Interaction energy (IE;  $\Delta E_{AB-C}$ ) was calculated by dividing the complex into two fragments, one consists of metal ion solvated by water molecules and the second fragment contains imidazole or methylimidazole with water molecules (see Scheme 2). Cooperativity ( $\Delta E_{\text{coop}}$ ) is computed by substituting different energy components obtained from eqs 2a–2d in Scheme 2.

## RESULTS AND DISCUSSION

In this section we begin with the discussion of energetics followed by structural analysis, charges, vibrational stretching frequencies, and AIM analysis. After that the biological relevance of metal ion–histidine complexes and role of solvent molecules in metal binding site are given. Although there are interesting subtle variations from metal to metal, upon sequential hydration the qualitative trends are essentially similar.

**Energetics.** The qualitative trends of IEs are essentially similar at the B3LYP and MP2 levels of theory. However, it was noticed that the IE values ( $\Delta E_{AB-C}$ ) are overestimated (by about 1–23 kcal/mol) at the B3LYP/6-311++G(d,p) level for smaller complexes, whereas for larger complexes the IEs are underestimated (by about 1–7 kcal/mol) with respect to the MP2(FULL)/6-311++G(d,p) level. Unless otherwise mentioned, all IEs are discussed on the basis of the MP2(FULL)/6-311++G(d,p) level. Computed IEs ( $\Delta E_{AB-C}$ ) of metal ions ( $\text{Li}^+$ ,  $\text{Na}^+$ , and  $\text{K}^+$ ) with imidazole are in very good agreement (within the deviation of 1–2 kcal/mol) with the experimental values (guided ion beam tandem mass spectrometer) reported by the groups of Rodgers and Ohanessian.<sup>7</sup> IEs presented in Table 1 reveals that some of the complexes (**Imi-1Wb** and **Imi-2Wc**) have higher IE values than **Imi-0W**. The complex **Imi-1Wb** has no water molecules attached to the metal, but it has one water molecule binding at N(1) through hydrogen bonding. For this complex, depending on the metal

Table 3. Calculated Interaction Energies of Metal Ions with Water, Imidazole, Methylimidazole, and Benzene

complex	$M = \text{Li}^+$	$M = \text{Na}^+$	$M = \text{K}^+$	$M = \text{Mg}^{2+}$	$M = \text{Cu}^+$	$M = \text{Zn}^{2+}$
$\text{M}-\text{H}_2\text{O}^a$	35.4	23.2	12.4	75.8	35.0 <sup>c</sup>	108.4 <sup>d</sup>
$\text{M}-\text{Imi}$	50.6	35.5	27.0	130.3	64.3	166.2
$\text{M}-\text{Me-Imi}$	53.0	37.4	28.9	136.5	69.3	179.1
$\text{M}-\text{Ben}^b$	33.7	20.4	16.3	107.6	51.1 <sup>c</sup>	

<sup>a</sup> Values are taken from ref 25c. <sup>b</sup> Values are taken from ref 2d. <sup>c</sup> Values are taken from ref 28. <sup>d</sup> Values are taken from ref 29.

ion, the IE value is about 5–21 kcal/mol higher than that of the **Imi-0W** complex. The complex **Imi-2Wc** has two water molecules near the imidazole moiety; for different metals present at the N(3) position of this complex, IEs increase by about 9.5–33 kcal/mol compared to that of the **Imi-0W** complex. As can be seen from Table 1, the increase in interaction energies depends on the nature of the metal ion present at the N(3) position of imidazole. Thus, for dicationic metal ion ( $\text{Mg}^{2+}$  and  $\text{Zn}^{2+}$ ) the increase in IE is about 33 kcal/mol, which is substantially higher than the monocationic one. Similarly, the complex **Imi-3Wc** shows about 4–16 kcal/mol increase in IE compared to **Imi-0W** complex for  $\text{Li}^+$  and  $\text{Cu}^+$  complexes, respectively. This complex has one water molecule coordinated with metal atom and the other two present near the imidazole motif. These results indicate that the presence of water molecules near the imidazole motif enhances the IEs of metal ion with N(3) of imidazole. The computed interaction energies for methylimidazole are shown in Table 2, and it can be seen that the qualitative trends of the IEs are similar for both imidazole and methylimidazole. The results show that the presence of methyl group at the C5 position slightly increases the IEs, which can be traced to the electron-donating nature of the methyl group present at the C5 position.

Computed hydrogen-bonding strengths at the N(1) position of imidazole and methylimidazole are plotted against the number of water molecules coordinated to the metal ions in each complex, and the correlation plots are depicted in Figure 1. The plots clearly indicate that the  $\text{O}\cdots\text{HN}(1)$  hydrogen-bond strength is a maximum when there is no water molecule coordinated to the metal ion, because as the coordination number of metal ion increases ( $m > 0$ ), the strength of the hydrogen bond gradually decreases. However, subtle variations are seen for  $\text{Li}^+$  and  $\text{Na}^+$  complexes when they are coordinated with four and five water molecules ( $m = 4$  and 5). These variations are due to the presence of one or more water

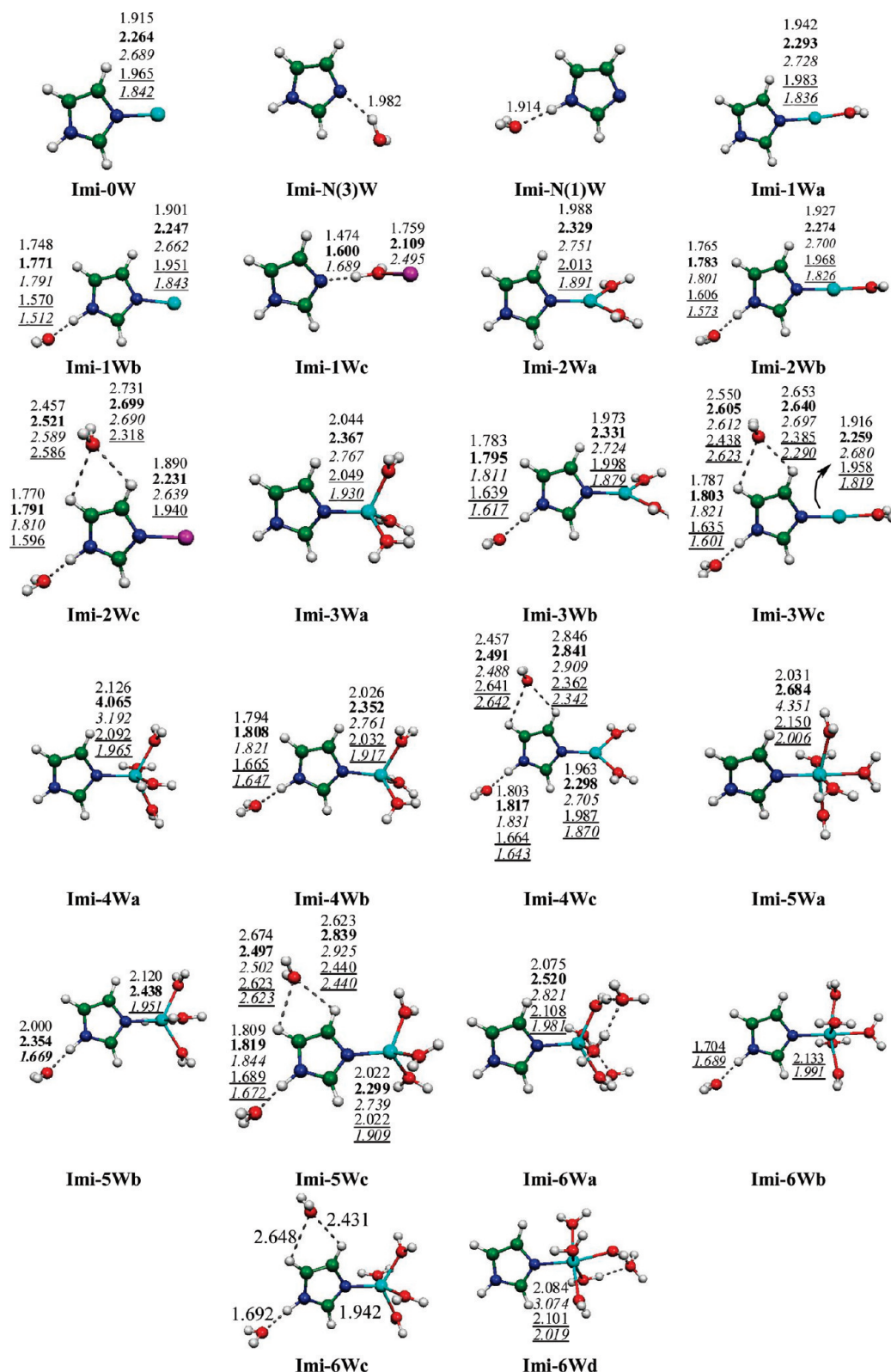


**Figure 4.** Geometrical parameters obtained at the B3LYP/6-31G(d,p) level for various complexes of solvated metal-imidazole complexes. Values are shown in normal type for Li<sup>+</sup>, bold for Na<sup>+</sup>, italic for K<sup>+</sup>, underlined for Mg<sup>2+</sup>, and underlined italics for Zn<sup>2+</sup> complexes. Bond lengths are given in Å.

molecules in their second solvation shell. Complexes of K<sup>+</sup> and Cu<sup>+</sup> with five water molecules ( $m = 5$ ) are found to be different from other metal complexes; in this case it is observed that some of the water molecules are positioned between the metal ion and imidazole

or methylimidazole (see **Imi-6Wb** for K<sup>+</sup> in Figure S5 of the Supporting Information). However, in the case of Cu<sup>+</sup>, due to extensive hydrogen bonding among the water molecules near the metal ion, the hydrogen bond gets strengthened. Figure 2 shows the

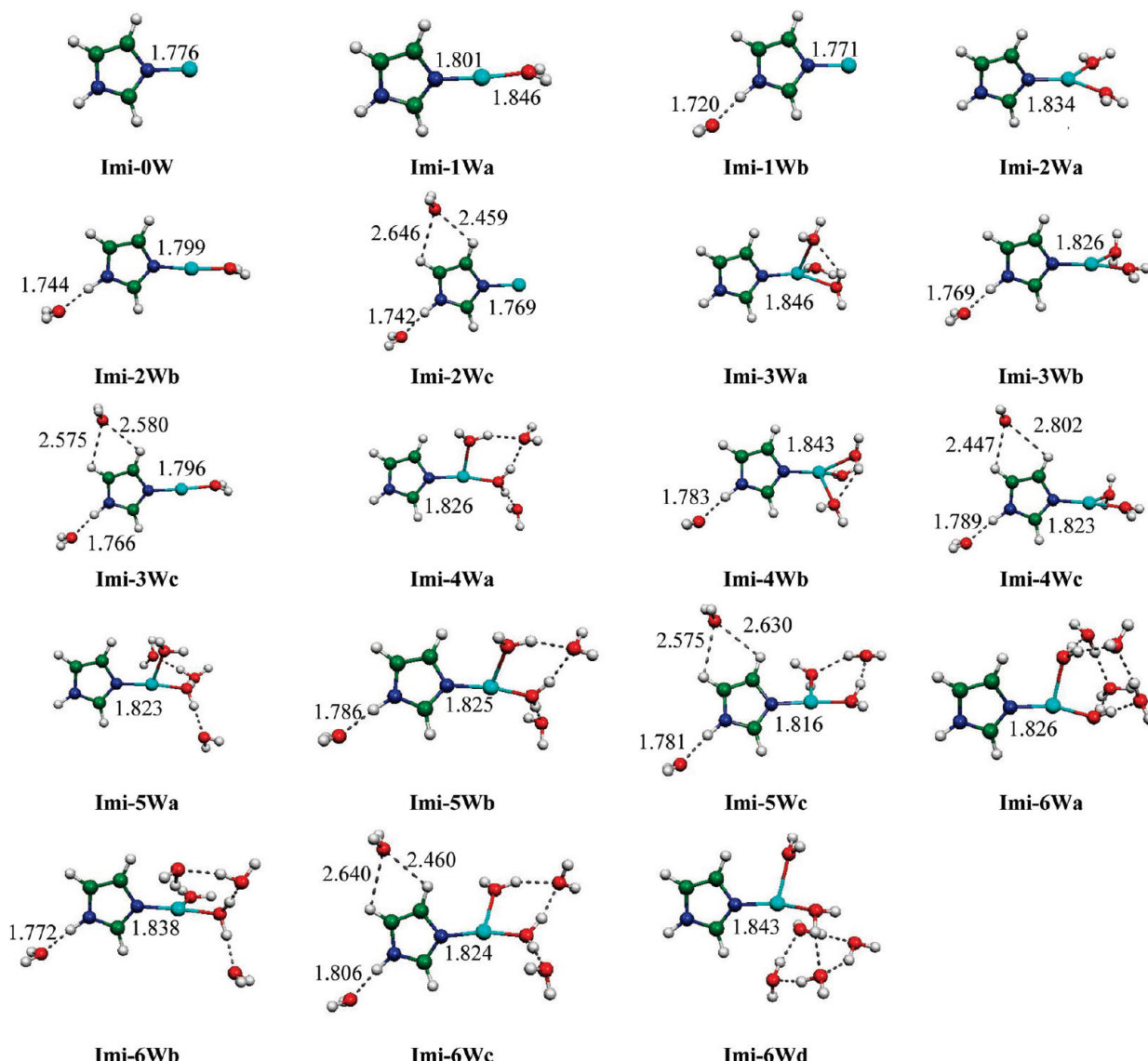


**Figure 5.** Geometrical parameters obtained at the B3LYP/6-31G(d,p) level for various complexes of solvated copper-imidazole complexes. Bond lengths are given in Å.

correlation plots of cooperativity versus number of water molecules coordinated to metal ions in imidazole and methylimidazole complexes. As can be noted from the plots, the cooperativity between the metal ion binding at the N(3) position and solvent at the N(1) position is a maximum when there are no water molecules coordinated with the metal ion. Upon the addition of water molecules to metal ion, the cooperativity values gradually decrease.

In one of our previous studies focused on the hydration effect on cation- $\pi$  complexation, we often witnessed a complete solvation of metal ion.<sup>10</sup> However, similar observations were not seen in the current study, this is because solvation of metal ion by breaking M–N contact is energetically not feasible (except for K<sup>+</sup> with six water molecules). The desolvation energy ( $\Delta E_{\text{Desolv}}$ ) is computed using Scheme 2, these energies are plotted against the number of water molecules coordinated with the metal ion, and the plots are available in Figure 3. The magnitude of desolvation energy provided an estimation of the relative preferences between imidazole and water for a given metal. As can be seen from the plots, the desolvation energy of Mg<sup>2+</sup> and Zn<sup>2+</sup> complexes decreases sharply up to  $m = 4$ , and thereafter, it is similar for all complexes. For Li<sup>+</sup> and

Na<sup>+</sup> complexes, the desolvation energy decreases monotonically with the increase of coordination number of metal ion. For  $m = 1$  and 2, the K<sup>+</sup> complexes also have shown results similar to those of Li<sup>+</sup> and Na<sup>+</sup> complexes; however, for  $m = 3$  and 4, a slight increase in desolvation energy is observed. It is noticed that the observed deviations are due to the simultaneous loss of hydrogen bonding among water molecules and the metal coordination in these (Imi-3Wa and Imi-4Wa; M = K<sup>+</sup>) complexes. The trends in desolvation energies of Cu<sup>+</sup> complexes are completely different from those of the other metals considered; this is because the arrangement of water molecules around this metal is slightly different from that of the other metals. Table 3 shows the interaction energies of metal ions with imidazole, methylimidazole, water, and benzene. From these values, it is clear that, compared to water, imidazole and methylimidazole have shown higher propensity to coordinate with the metal ions. Therefore, one of the coordination sites of solvated metal ion can be easily replaced by a histidine side chain.

**Geometries.** Figures 4 and 5 show the optimized geometries of hydrated Imi-M (where M = Li<sup>+</sup>, Na<sup>+</sup>, K<sup>+</sup>, Mg<sup>2+</sup>, Cu<sup>+</sup>, and Zn<sup>2+</sup>) complexes at the B3LYP/6-31G(d,p) level. The

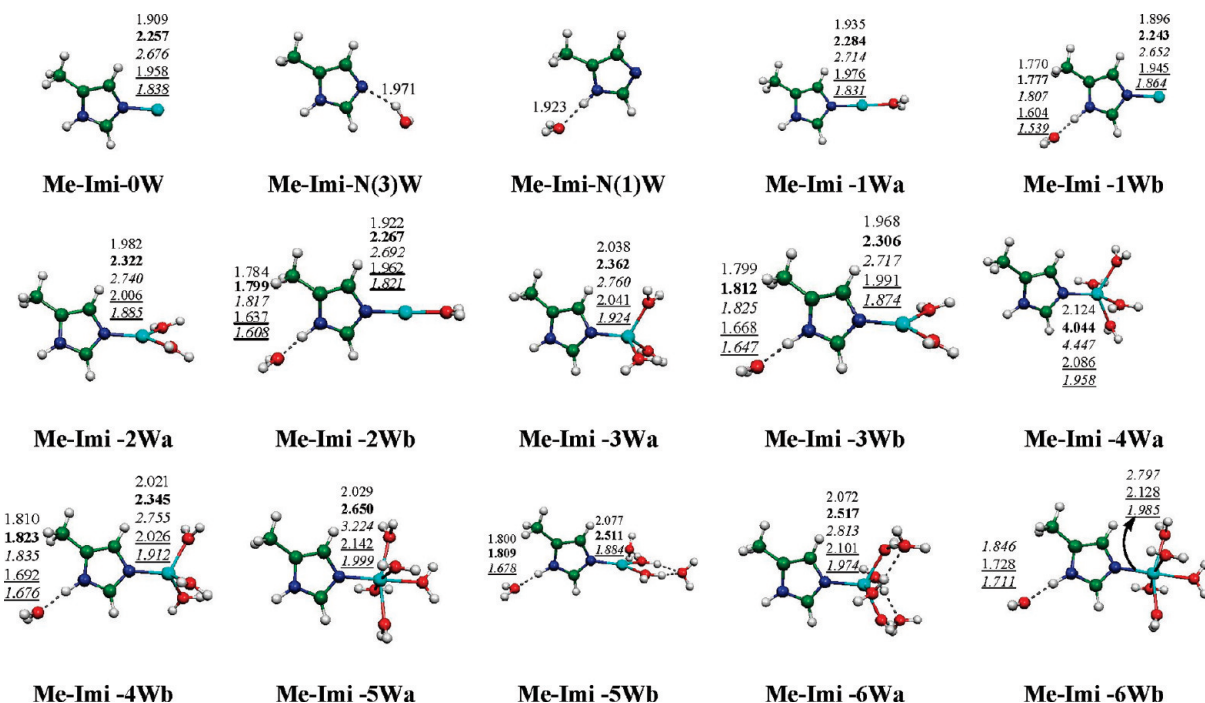


Figure 6. Geometrical parameters obtained at the B3LYP/6-31G(d,p) level for various complexes of solvated metal–methylimidazole complexes. Values are shown in normal type for  $\text{Li}^+$ , bold for  $\text{Na}^+$ , italic for  $\text{K}^+$ , underlined for  $\text{Mg}^{2+}$ , and underlined italics for  $\text{Zn}^{2+}$  complexes. Bond lengths are given in Å.

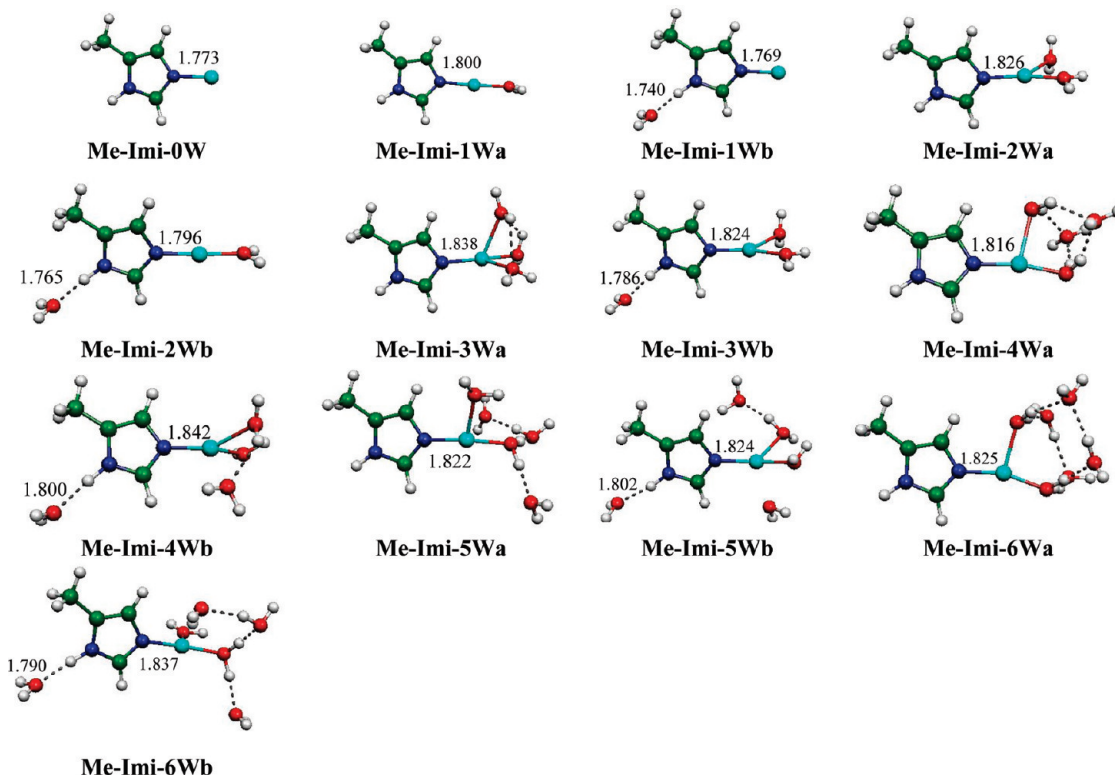


Figure 7. Geometrical parameters obtained at the B3LYP/6-31G(d,p) level for various complexes of solvated copper–methylimidazole complexes. Bond lengths are given in Å.

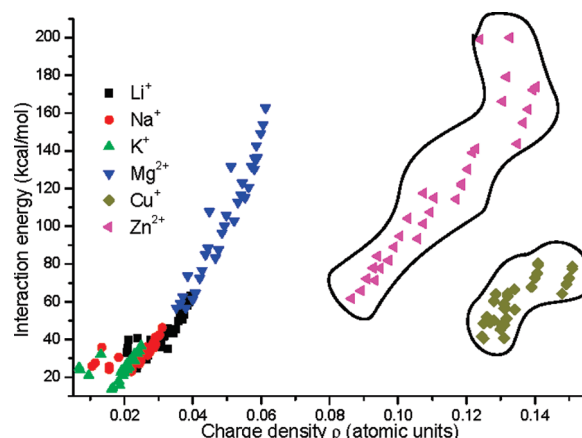
geometries for  $\text{Cu}^+$  complexes are different from the other metal ions considered, and hence, they have been presented differently in Figures 5 and 7. To gauge the structural changes upon the hydration of metal–imidazole or–methylimidazole complexes,

water molecules are sequentially added to both metal as well as imidazole or methylimidazole. The distance between the metal ion and the N(3) of imidazole is considered a cation– $\sigma$  distance and is used throughout the discussion. The cation– $\sigma$  distance

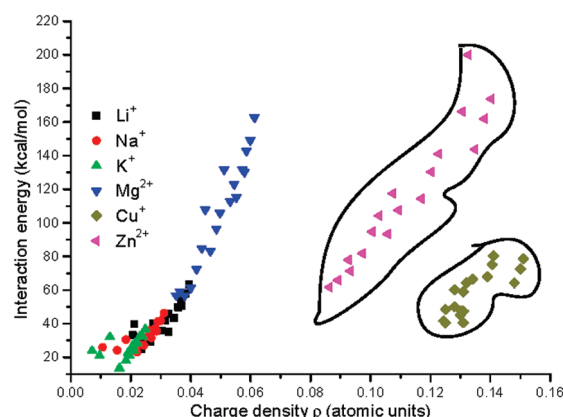
without any solvent molecules around the system is noted as 1.915 Å for the  $\text{Li}^+$  complex. Expectedly, sequential addition of water molecules to metal ion probably elongates the cation– $\sigma$  distance. Previous studies demonstrated that the  $\text{Li}^+$  and  $\text{Na}^+$  can accept four water molecules in its first coordination shell; the coordination number is four.<sup>25</sup> In this study, we forced the fifth coordination with N(3) of imidazole or methylimidazole; however, these complexes are found to be higher order saddle points on potential energy surface. Attempts to get the minimum energy complex resulted in a conformation wherein one of the water molecules was pushed to the second solvation shell of the metal ion. The cation– $\sigma$  distance is lengthening from 1.915 to 2.157 Å when the metal ion is coordinated with four water molecules. The complexes Imi-*n*Wb and Imi-*n*Wc (*n* = 1–6) have shown dramatic changes in their structural features upon introducing the solvent molecules near the imidazole or methylimidazole motifs.

The presence of a metal ion at the N(3) position shortens the O···HN(1) bond distance, and vice versa. For  $\text{K}^+$  complexes with five and six (*m* = 4 and 5) water molecules, the structural features are completely different from the other metals considered. In the case of *m* = 4, four water molecules form a hydrogen-bonding network and interact with potassium from one face, and the imidazole is coordinated from the opposite face of the  $\text{K}^+$ . For *m* = 5, some of the water molecules come between N(3) of imidazole or methylimidazole and  $\text{K}^+$ .

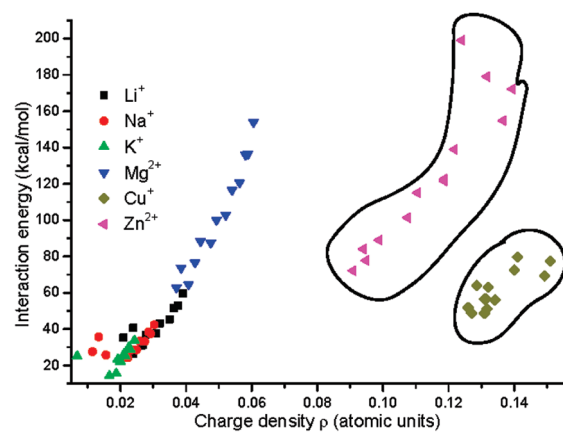
For  $\text{Mg}^{2+}$  complexes, depending on the number of solvent molecules, the cation– $\sigma$  distance varies from 1.965 to 2.202 Å, respectively. Similar to  $\text{Li}^+$  and other monovalent metal complexes, if the solvent molecules are present near the imidazole ring, the cation– $\sigma$  distances get shortened. During the solvation of Imi–M (M =  $\text{Li}^+$ ,  $\text{Na}^+$ , and  $\text{K}^+$ ) we could locate complexes wherein two water molecules attached to the imidazole ring through hydrogen bonding. The first one forms hydrogen bonding with hydrogen atoms present on the N(1) atom and the second water for the C–H···O type of hydrogen bonding with hydrogens present on C(4) and C(5) atoms. A similar complex for the solvation of Imi–Mg could not be located on the potential energy surface; the trials for locating this complex lead to the Imi-2Wa type of complex. In order to achieve these complexes, geometry optimizations are carried out by freezing the C(4)–H···O and C(5)–H···O distances. Similar to  $\text{Li}^+$  and  $\text{Na}^+$ , Imi-5Wb and Imi-6Wa type of complexes could be located for  $\text{Mg}^{2+}$ ; in these complexes  $\text{Mg}^{2+}$  is solvated with three and four water molecules, respectively. The current study also reports about the complexes wherein solvent molecules are present in between the metal ion and N(3) of imidazole (see Imi-1Wc in Figure 4). Comparison of hydrogen bond distances in Imi-1Wc and Imi-N(3)W reveals that the  $\text{Li}^+$ ,  $\text{Na}^+$ , and  $\text{K}^+$  can enhance the proton-donating capacity of water molecule to form hydrogen bonds with the N(3) of imidazole. Similar complexes could not be located for  $\text{Cu}^+$ ,  $\text{Mg}^{2+}$ , and  $\text{Zn}^{2+}$ . Replacing  $\text{Li}^+$  with  $\text{Mg}^{2+}$  leads to protonated imidazole and Mg–OH. The geometrical parameters for all methylimidazole–metal complexes are shown in Figures 6 and 7. Depending on the number of water molecules attached to the  $\text{Cu}^+$  and  $\text{Zn}^{2+}$  ion, the cation– $\sigma$  distance for the  $\text{Cu}^+$  complexes varies from 1.776 to 2.846 Å. The  $\text{Cu}^+$  complexes show the shortest cation– $\sigma$  distance among all metal ion complexes considered in this study. However, the other complexes are formed mainly due to the noncovalent interactions that have longer distances compare to  $\text{Cu}^+$  complexes. These differences in the nature of bonding are also reflected in the binding energies in which  $\text{Cu}^+$  and  $\text{Zn}^{2+}$  have higher interaction



a



b



c

**Figure 8.** Correlation of interaction energies with the charge densities at bond critical points at M–N(3): (a) imidazole and methylimidazole with all metals considered, (b) imidazole with all metals, and (c) methylimidazole with all metals considered.

energies compare to other mono- and divalent metal ions considered. Comparatively, M–N(3) distances in methylimidazole are slightly shorter than in imidazole; this is because of the electron-donating nature of the methyl group present at the C5 position.

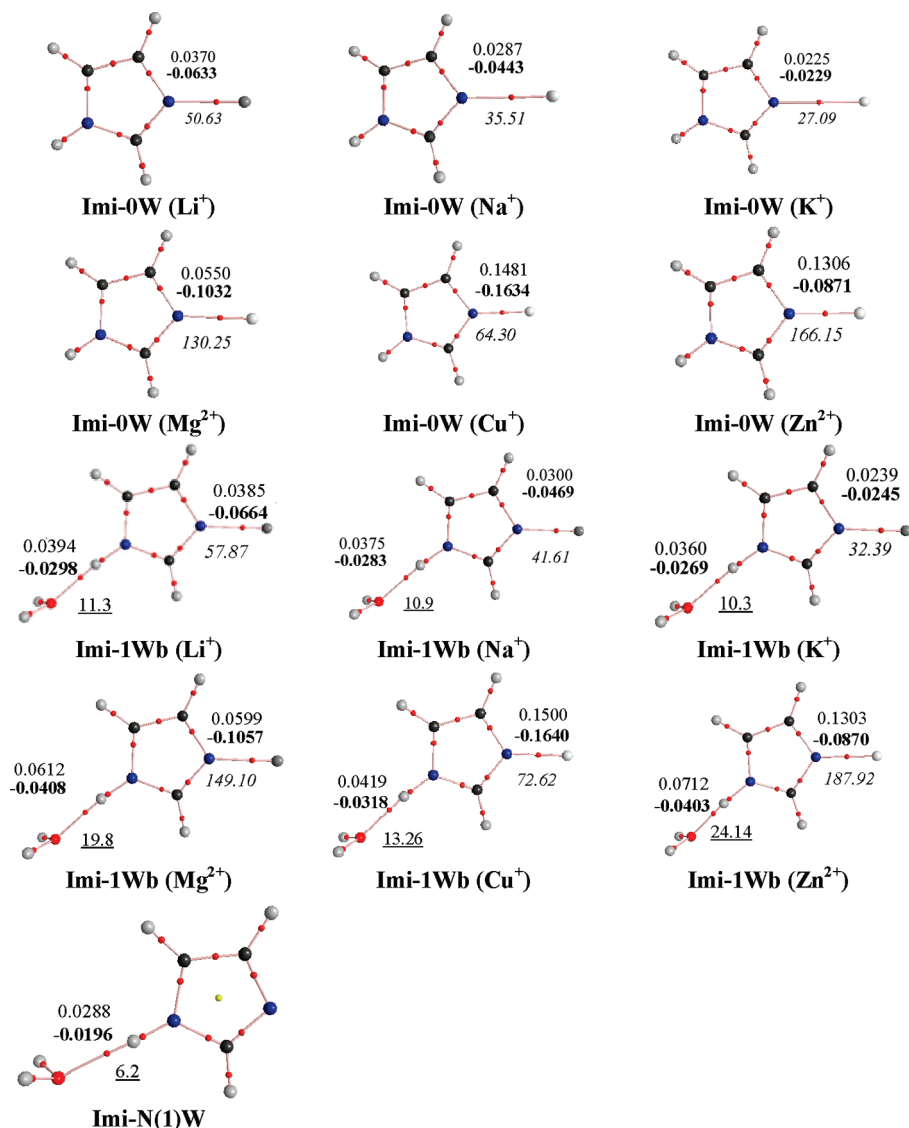


**Figure 9.** AIM topological plots obtained for metal-imidazole, imidazole-water, and metal-imidazole with one water complexes. Charge density (normal) and Laplacians (bold) values at bond critical points are given in atomic units. Values presented in italics are the IEs in kcal/mol ( $\Delta E_{AB-C}$ ) and underlined values are the hydrogen-bonding strength at the N(1)-H $\cdots$ O bond.

**Charge Analysis.** Partial atomic charges obtained using the NPA method at the HF/6-311++G(d,p) level for Imi-M (M = Li<sup>+</sup>, Na<sup>+</sup>, K<sup>+</sup>, Mg<sup>2+</sup>, Cu<sup>+</sup>, and Zn<sup>2+</sup>) complexes are depicted in Tables S3 and S4 of the Supporting Information. From the charges presented in the tables it is clear that, if the coordination number of metal ion increases, the charge on metal ion decreases monotonically. Addition of water molecule at the N(1) position makes the N(3) nitrogen more negative in Imi-0w, Imi-1Wb, and Imi-2Wc complexes; consequently, these complexes show high charge transfer from N(3) to the metal ion. The complexes mentioned above have shown maximum IE among all complexes considered in the current study. It is clearly observed that the presence of solvent molecule at the N(1) position of imidazole through hydrogen bonding enhances the charge on the N(3) nitrogen, which in turn increases the IE of metal ions with N(3). This effect is more significant in the case of Mg<sup>2+</sup> and Zn<sup>2+</sup> complexes. These observations show that the metal ion binding at the N(3) position and the solvent binding at the N(1) position have cooperative effects to enhance their binding with the

imidazole ring. For transition metal ion complexes, the charge transfer from N(3) to metal ions was found to be more than that of alkali and alkaline earth metal complexes. For Cu<sup>+</sup> complexes, until  $m = 3$ , the net charge transfer is higher compared to that of other monovalent cations. However, once the water molecules coordinate to the metal ions, the cooperative effect gets diminished and the charge transfer takes place mostly between the solvent molecules and the metal ions.

**Atoms in Molecule Analysis.** The results of AIM analysis for different  $m$  and  $n$  values of imidazole and methylimidazole complexes are depicted in Tables S5 and S6 of the Supporting Information. From these results it is clear that, when  $n$  is kept constant and the  $m$  value is increased, then the electron densities at bond critical points (BCPs; N(3)-M, M = Li<sup>+</sup>, Na<sup>+</sup>, K<sup>+</sup>, Mg<sup>2+</sup>, Cu<sup>+</sup>, and Zn<sup>2+</sup>) are gradually decreasing. However, if the value of  $n$  is increased from 0–2, higher charge densities are observed at the BCPs. Transition metal ion complexes showed higher charge density at the bond critical point than their alkali and alkaline earth metal ion analogues. Between Cu<sup>+</sup> and Zn<sup>2+</sup>

**Table 4.** N–H Stretching Frequencies in  $\text{cm}^{-1}$  Obtained for Imidazole and Methylimidazole at the B3LYP/6-31G(d,p) Level of Theory

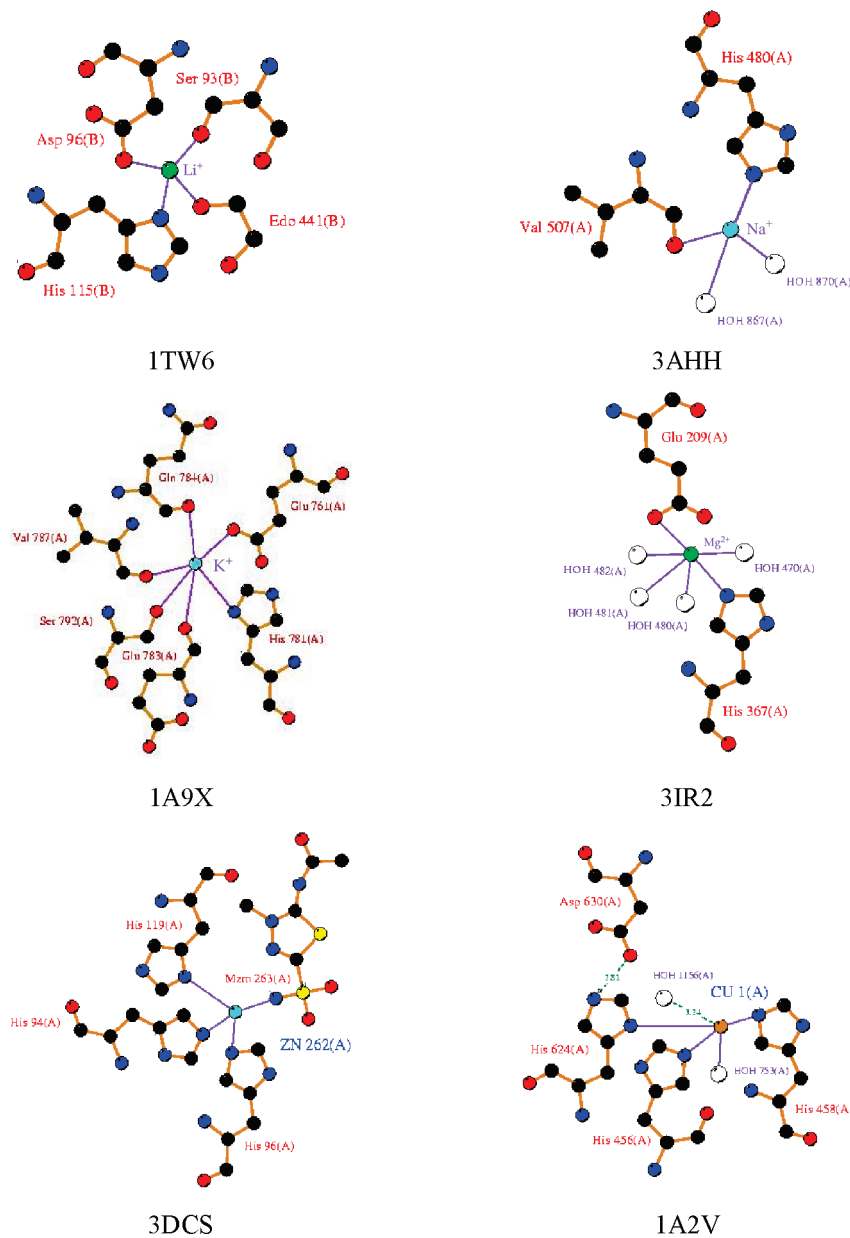
complex	M = Li <sup>+</sup>	M = Na <sup>+</sup>	M = K <sup>+</sup>	M = Mg <sup>2+</sup>	M = Cu <sup>+</sup>	M = Zn <sup>2+</sup>
Imi	3523.69	3523.69	3523.69	3523.69	3523.69	3523.69
Imi-0W	3502.56	3506.87	3510.15	3436.09	3498.97	3416.62
Imi-N(1)W	3339.61	3339.61	3339.61	3339.61	3339.61	3339.61
Imi-1Wb	3120.55	3162.71	3196.93	2582.76	3063.44	2338.79
Imi-2Wb	3155.55	3185.13	3213.84	2718.76	3117.62	2602.48
Imi-2Wc	3161.56	3197.61	3228.01	2692.93	3109.50	2537.56
Imi-3Wb	3185.91	3206.26	3228.73	2824.20	3163.61	2758.80
Imi-3Wc	3193.24	3218.16	3244.22	2809.80	3157.99	2700.94
Imi-4Wb	3202.49	3226.15	3241.62	2901.55	3185.77	2853.20
Imi-4Wc	3218.16	3236.88	3257.57	2897.84	3199.76	2837.81
Imi-5Wb	3185.67	3209.88	3213.50	2950.43	3198.79	2913.39
Imi-5Wc	3228.36	3242.17	3240.60	2966.09	3188.73	2920.64
Imi-6Wb	3230.57	3211.27	3194.70	3002.57	3171.83	2962.29
Imi-6Wc	<sup>a</sup>	<sup>a</sup>	<sup>a</sup>	3006.41	3229.95	2971.93
Me-Imi	3375.01	3375.01	3375.01	3375.01	3375.01	3375.01
Me-Imi-0W	3497.61	3501.24	3504.09	3438.84	3494.47	3420.72
Me-Imi-N(1)W	3208.41	3208.41	3208.41	3208.41	3208.41	3208.41
Me-Imi-1Wb	3157.42	3175.62	3219.58	2699.90	3105.47	2464.14
Me-Imi-2Wb	3184.28	3208.80	3234.33	2813.47	3154.52	2718.17
Me-Imi-3Wb	3210.32	3228.26	3246.99	2904.05	3193.18	2847.18
Me-Imi-4Wb	3223.63	3244.69	3258.02	2968.01	3209.15	2927.37
Me-Imi-5Wb	3207.16	3223.89	3232.78	3007.88	3221.56	2937.68
Me-Imi-6Wb	3205.24	3228.81	3237.91	3052.19	3199.62	3015.21

<sup>a</sup> The corresponding alkali metal complexes are not minima on the potential energy surface.

complexes, the charge density was found to be more for Cu<sup>+</sup> complexes. Thus, Cu<sup>+</sup>–imidazole or –methylimidazole interaction is of more covalent character. The charge densities obtained at bond critical points [M–N(3)] are plotted against the interaction energies ( $\Delta E_{\text{AB-C}}$ ), and the plots are given in Figure 8. Plots presented here have clearly showed that the charge densities at bond critical points are directly proportional to the interaction energies, except for Cu<sup>+</sup>, which may be due to a higher admixture of covalent character. Correlation plots are made in the following way: plot a shows the correlation of interaction energies for all metals and two bases with the charge densities, plot b shows the correlation of interaction energies obtained for all metals with imidazole and the corresponding charge densities, and finally plot c shows the correlation of interaction energies of methylimidazole complex with corresponding charge densities. From these plots, it is clear that the charge densities are higher for complexes with higher IEs, correlation coefficient values being more or less similar in all the cases. For selected complexes, the molecular graphs obtained from AIM analysis are given in Figure 9. As evident from Figure 9, the charge density obtained at bond critical points of the O···HN-(1) hydrogen bond in the absence of metal ion at N(3) is 0.0288 au [see Imi-N(1)W complex in Figure 9]. The presence of metal ion at N(3) shows a dramatic effect on the charge density at O···HN(1), depending on the metal ion charge density at BCP of O···HN(1), varying from 0.0394 to 0.0712 au. This shows that the metal ion at the N(3) position strongly influences the hydrogen bonding at the N(1) position of imidazole. For the bond critical points at M–N(3), expectedly solvation of metal ion decreases the charge density at their BCPs. However, the complexes **Imi-1Wb**, **Imi-2Wb**, and **Imi-2Wc** have higher charge density at the bond critical points than bare **Imi-0W** (without solvent) complex. In all these complexes one water molecule is attached at the N(1) position through hydrogen bonding. It can be seen from Figure 8 that the metal ion at the N(3) position of the imidazole ring strongly influences the N(1)–H···O hydrogen bonding. Imidazole solvated

with one water molecule at the N(1) position has a hydrogen bond strength of 6.2 kcal/mol, and the electron charge density at the BCP is 0.0288 au. The presence of Li<sup>+</sup> at the N(3) position strengthened the hydrogen bond by about 5 kcal/mol, and correspondingly, the electron charge density at BCP is increased to 0.0385 au. The presence of Mg<sup>2+</sup> at N(3) increases the strength of the N(1)–H···O hydrogen bond by about 16 kcal/mol, and the presence of Zn<sup>2+</sup> at N(3) increases it by 18 kcal/mol. The observed changes in the electron densities are due to the strong electron-withdrawing nature of metal ions present at the N(3) atom.

**Vibrational Stretching Frequencies.** In this section we seek to explore whether the variations in the hydrogen-bond strengths upon metal ion binding and sequential hydrations are reflected in their vibrational stretching frequencies. This is done by considering the most important N–H stretching frequency of the imidazole motif. Vibrational stretching frequencies of N–H of imidazole and methylimidazole computed using B3LYP/6-31G(d,p) level are shown in Table 4. N–H stretching frequency varies by either the presence of metal ion at N(3) or water at N(1). The computed N–H stretching frequency of imidazole, 3523 (with a scaling factor 0.96),<sup>26</sup> is in excellent agreement with the experimental values of 3518–3504  $\text{cm}^{-1}$ .<sup>27</sup> Thus, the computational method employed here is reliable, and we here report the frequencies, which are scaled by a factor of 0.96. The presence of metal ion shows a clear shift in the N–H stretching frequencies, as represented in Table 4; depending on the metal ion, stretching frequencies lower by 13.0–107  $\text{cm}^{-1}$ . This observation clearly indicates that the presence of metal ion at the N(3) position attenuates the N–H proton to participate in the hydrogen bonding. Similarly, the presence of solvent molecule at the N(1)–H position shifts the N–H stretching frequency from 3523.69 to 3339.61  $\text{cm}^{-1}$ . From the above observations it can be understood that both metal ion at N(3) and solvent molecules at N(1) position mutually cooperate with each other in binding at their respective binding sites of imidazole. As the coordination number of metal ion increases ( $m > 0$ ), a slight

Scheme 3. Snapshots Taken from Different Proteins Containing Metal–Histidine Complexes<sup>a</sup>

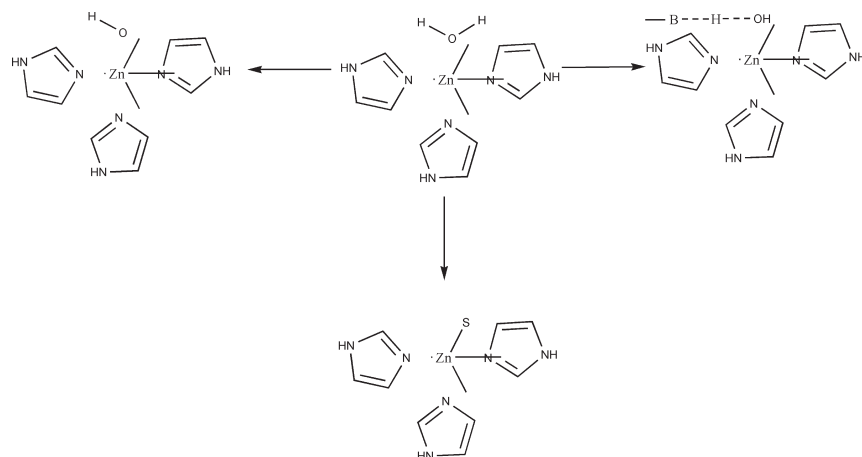
<sup>a</sup> Under each complex the PDB ID is given.

shift in the stretching frequencies is noticed. Except subtle variations in the quantities of stretching frequencies of imidazole and methylimidazole, the qualitative trends are identical to each other; thus, the discussion is restricted to imidazole only.

**Biological Relevance.** Model systems considered in the study were conceived due to their relevance to biomacromolecules. Metal ions play a pivotal role in the functions of metalloproteins. The selectivity of metal ions for specific proteins is governed by the several factors, and the role of solvent molecules in the metal ion active sites is a subject of great interest. Many histidine-rich sites in proteins bind to transition metal ions, which control protein folding and are important for the enzymatic capabilities, such as hydrolysis, dioxygen transport, and electron transfer. For example, the metal ions Cu<sup>2+</sup>, Zn<sup>2+</sup>, and Fe<sup>3+</sup> are known to be involved in the oxidation process of methionine (position 35) of amyloid  $\beta$  peptide

by complexing to the imidazole (positions 13 and 14) of the same peptide.<sup>28</sup> Density functional calculations (DFT) illustrated that the hydrated transition metal ion complexes of the histidine side chain of amyloid  $\beta$  peptide catalyzes the oxidation of methionine through a concerted mechanism.<sup>28</sup> Analyzing the protein crystal structures was a great source of the information to understand the structure–activity relationship. This analysis motivated us to search for the available metalloproteins in the Protein Data Bank (PDB), where the metal ions are partially solvated and have bound histidine residue. Metal histidine complexes are highly abundant in nature, and protein crystal structure data indicate that such complexes are available with essentially most metals considered in the study. Metal ions not only determine the catalytic activity of proteins but also determine the stability of DNA duplex, depending on the modes of binding and the nature of the metal ions.<sup>29</sup> Scheme 3 depicts the representative

**Scheme 4. Schematic Representation of the Functions of Active Water Present in the Active Site of Carbonic Anhydrase Isozyme IX**



snapshots for each of the metal ion considered in the study. A large number of such structures are available with essentially all metal ions. Obviously, these metal ions play extremely important functional and regulatory roles in biomacromolecules. Identification and characterization of the metal ions are important and interesting in their own right.<sup>30</sup> Carbamoyl phosphate synthetase (CPS) from *Escherichia coli* belongs to glutamine amidotransferase class of enzymes, as it involves in the catalytic formation of carbamoyl phosphate. CPS has two polypeptide chains, where the larger one provides the active site and the small chain catalyzes the hydrolysis of glutamine to glutamate and ammonia. In the larger chain, carbamoyl phosphate is synthesized from two molecules of Mg<sup>2+</sup>ATP, one molecule of bicarbonate, and one molecule of glutamine.<sup>31</sup>

Superoxide dismutases (SODs) are a class of enzymes that catalyze the dismutation of superoxide into oxygen and hydrogen peroxide. They are an important antioxidant defense in nearly all cells exposed to oxygen. To date, three major families of SODs have been discovered and among them copper–zinc superoxide dismutases (CuZnSOD) are most common in all eukaryotes. Earlier theoretical and experimental results for the electron transfer mechanism in CuZnSOD show that the fluctuations in the protein solvent environment are essential to understand the concerted rupture of the copper–histidine coordination-bond and the copper–superoxide bond in the active site. In CuZnSOD the active metal is Cu; i.e., Cu plays an essential role in enzymatic behavior, whereas Zn atom acts as a structural stabilization factor.<sup>32</sup>

Carbonic anhydrases are zinc–metalloenzymes that catalyze the hydration and dehydration of carbon dioxide and bicarbonate, respectively. The  $\alpha$ -class of anhydride is mostly present in vertebrates, where the Zn ion is tetravalently coordinated to three imidazole rings and one water molecule is the active site and the zinc ion is located at the bottom of the conical active site cavity. Carbonic anhydrase isozyme IX belongs to the  $\alpha$ -class and it has been found that in some cancers overexpression of carbonic anhydrase isozyme IX promotes growth and metastasis of the tumor, which makes it a good target for cancer treatment. In this protein, water is acting as the fourth ligand and as a critical component. This water can be activated by ionization or polarization or made available for displacement, as shown in Scheme 4. It has been suggested that the mechanistic pathway for activating

the water depends on the identity of the other three ligands coordinated to zinc ion and their spacing.<sup>33</sup> ML-IAP is an anti-apoptotic protein actively regulating the apoptosis in melanoma. L-Phenylalanine dehydrogenase from *Rhodococcus* species is an oxidoreductase catalyzing the conversion of phenylalanine to phenyl pyruvate. The above examples provide only a few sample cases for the myriad ways in which metal ions play an important role in biological systems, and it should be amply clear that they play an extremely diversified and important role in determining biological structure and function. Clearly, the effect and role of solvated water in metal ion complexes is profound and is a topic of outstanding importance and relevance in understanding biological processes.<sup>34</sup>

## CONCLUSIONS

Alkali, alkaline earth metal, and transition metal ions binding to imidazole and methyl imidazole motifs, which model the histidine side chain, have a strong preference to bind to the lone pair of nitrogen, and solvation plays an important role in the structure and dynamics of these complexes. Explicit solvent effects were analyzed on the metal ion complexation by taking water molecules that virtually fill the first solvation shell. The metal ions show higher propensity to bind to the imidazole motif compared to water or benzene, and therefore, it was not surprising that histidine is the most ubiquitous amino acid residue in metal binding sites. The study carefully analyzes hydrogen-bond-donating abilities of the N–H group of histidine upon unsolvated and solvated metal ion binding to its other nitrogen [N(3)] center. The study ensures that the first solvation shell is satisfied for all metal ion complexes. The presence of solvent molecules at the N(1) position of imidazole or methylimidazole enhances the metal ion binding at the N(3) position, and the binding of metal ion at the N(3) position strengthens the hydrogen bonding at the N(1) position. The shift in the vibrational frequencies of N–H indicates that the presence of metal ion at the N(3) position strengthens the hydrogen bond at the N(1) position. The charge densities obtained at bond critical points confirm the observed variations in the IE upon the solvation of different considered complexes. The study demonstrates a higher cooperative effect in the hydrogen bonding due to

transition metal ions compared to alkali and alkali earth metals. The current study brings out the significance of incorporating the metal ions in modeling the biomolecules.

## ■ ASSOCIATED CONTENT

**S Supporting Information.** Geometrical parameters of  $\text{Li}^+$ ,  $\text{Na}^+$ ,  $\text{K}^+$ ,  $\text{Mg}^{2+}$ ,  $\text{Cu}^+$ , and  $\text{Zn}^{2+}$  complexes at the B3LYP/6-31G(d,p) level; total energies of all considered complexes at MP2(FULL)/6-311++G(d,p) and B3LYP/6-31++G(d,p) levels; and computed NPA charges at the HF/6-311++G(d,p) level. Optimized geometries of all considered complexes can be obtained from authors upon request. This material is free of charge via Internet at <http://pubs.acs.org>.

## ■ AUTHOR INFORMATION

### Corresponding Author

\*E-mail: gnsastry@gmail.com

## ■ ACKNOWLEDGMENT

A. S. Reddy is thanked for his help and comments. We thank DAE-BRNS and DST for financial support in the form of Swarnajayanti Fellowship (to G.N.S.). B.S. thanks CSIR, New Delhi, JRF, CSIR network project (NWP053) center for excellence is thanked for financial assistance.

## ■ REFERENCES

- (1) Eller, K. *Organometallic Ion Chemistry*; Freiser, B. S., Ed.; Kluwer: Amsterdam, 1996; p 123. *Metal Ions in Biology and Medicine*; Etienne, J. C., Khassanovc, Z., Maynard, I., Collery, P., Khassanova, L., Eds.; Eurotext: Paris, 2002; Vol. 7 and previous volumes.
- (2) (a) Dougherty, D. A.; Stauffer, D. A. *Science* **1990**, *250*, 1558. (b) Kumpf, R. A.; Dougherty, D. A. *Science* **1998**, *261*, 1708. (c) Ma, J. C.; Dougherty, D. A. *Chem. Rev.* **1997**, *97*, 1303. (d) Gallivan, J. P.; Dougherty, D. A. *J. Am. Chem. Soc.* **2000**, *122*, 870. (e) Gallivan, J. P.; Dougherty, D. A. *Proc. Natl. Acad. Sci. U.S.A.* **1999**, *96*, 9459. (f) Crowley, P. B.; Golovin, A. *PROTEINS: Struct. Funct. Bioinfo.* **2005**, *59*, 231. (g) Chipot, C.; Maigret, B.; Pearlman, D. A.; Kollman, P. A. *J. Am. Chem. Soc.* **1996**, *118*, 2998.
- (3) (a) Wall, S. L. D.; Meadows, E. S.; Barbour, L. J.; Gokel, G. W. *Proc. Natl. Acad. Sci. U.S.A.* **2000**, *97*, 6271. (b) Hu, J.; Barbour, L. J.; Gokel, G. W. *Proc. Natl. Acad. Sci. U.S.A.* **2002**, *99*, 5121.
- (4) (a) Suelter, C. *Science* **1970**, *168*, 789. (b) McRee, D. E. *Nat. Struct. Biol.* **1998**, *5*, 8. (c) Hong, B. H.; Bae, S. C.; Lee, C. W.; Jeong, S.; Kim, K. S. *Science* **2001**, *294*, 348. (d) Kim, K. S.; Tarakeshwar, P.; Lee, J. Y. *Chem. Rev.* **2000**, *100*, 4145. (e) Tatko, C.; Waters, M. L. *Protein Sci.* **2003**, *12*, 2443. (f) Sunner, J.; Nishizawa, K.; Kebarle, K. *J. Phys. Chem.* **1961**, *65*, 1814. (g) Deakynet, C. A.; Mautner, M. *J. Am. Chem. Soc.* **1985**, *107*, 474.
- (5) (a) Huang, H.; Rodgers, M. T. *J. Am. Chem. Soc.* **2002**, *106*, 4277. (b) Vijay, D.; Sastry, G. N. *J. Phys. Chem. A* **2006**, *110*, 10148.
- (6) Dunbar, R. C.; Polfer, N. C.; Oomens, J. *J. Am. Chem. Soc.* **2007**, *129*, 14562.
- (7) (a) Huang, H.; Rodgers, M. T. *J. Am. Chem. Soc.* **2002**, *106*, 4277. (b) Kapota, C.; Ohanessian, G. *Phys. Chem. Chem. Phys.* **2005**, *7*, 3744. (c) Wang, P.; Wesdemiotisa, C.; Kapota, C.; Ohanessian, G. *J. Am. Soc. Mass Spectrom.* **2007**, *18*, 541. (d) Hoyau, S.; Norrman, K.; McMahon, T. B.; Ohanessian, G. *J. Am. Chem. Soc.* **1999**, *121*, 8864.
- (8) (a) Bush, M. F.; Oomens, J.; Saykally, R. J.; Williams, E. R. *J. Am. Chem. Soc.* **2008**, *130*, 6463. (b) Bush, M. F.; Prell, J. S.; Saykally, R. J.; Williams, E. R. *J. Am. Chem. Soc.* **2007**, *129*, 13544.
- (9) (a) Strittmatter, E. F.; Wong, R. L.; Williams, E. R. *J. Phys. Chem. A* **2000**, *104*, 9793. (b) Rodriguez-Cruz, S. E.; Jockusch, R. A.; Williams, E. R. *J. Am. Soc. Mass Spectrom.* **2001**, *12*, 250. (c) Blom, M. N.; Compagnon, I.; Polfer, N. C.; Helden, G. V.; Meijer, G.; Suhai, S.; Païzs, B.; Oomens, J. *J. Phys. Chem. A* **2007**, *111*, 7309. (d) Wouters, J. *Protein Sci.* **1998**, *7*, 2472. (e) Wu, R.; McMahon, T. B. *J. Am. Chem. Soc.* **2008**, *130*, 12554.
- (10) (a) Rao, J. S.; Zipse, H.; Sastry, G. N. *J. Phys. Chem. B* **2009**, *113*, 7225. (b) Reddy, A. S.; Zipse, H.; Sastry, G. N. *J. Phys. Chem. B* **2007**, *111*, 11546. (c) Mahadevi, A. S.; Sastry, G. N. *J. Phys. Chem. B* **2011**, *115*, 703.
- (11) (a) Reddy, A. S.; Sastry, G. N. *PROTEINS: Struct. Funct. Bioinfo.* **2007**, *67*, 1179. (b) Reddy, A. S.; Sastry, G. N. *J. Phys. Chem. A* **2005**, *109*, 8893.
- (12) (a) Chelli, R.; Procacci, P. *J. Phys. Chem. B* **2006**, *110*, 10204. (b) Chakrabarti, P. *Protein Eng.* **1990**, *4*, 57.
- (13) (a) Bebrane, C.; Delbrück, H.; Kupper, M. B.; Schloemer, P.; Willmann, C.; Frere, J.; Fischer, R.; Galleni, M.; Hoffmann, K. M. V. *Antimicrob. Agents Chemother.* **2009**, *53*, 4464. (b) Leitgeb, S.; Nidetzky, B. *Biochem. Soc. Trans.* **2008**, *36*, 1180.
- (14) (a) Rao, J. S.; Sastry, G. N. *J. Phys. Chem. A* **2009**, *113*, 5446. (b) Lemoff, A. S.; Bush, M. F.; Wu, C. C.; Williams, E. R. *J. Am. Chem. Soc.* **2005**, *127*, 10276. (c) Polfer, N. C.; Oomens, J.; Dunbar, R. C. *Chem. Phys. Chem.* **2008**, *9*, 579. (d) Ryzhov, V.; Dunbar, R. C.; Cerda, B.; Wesdemiotis, C. *J. Am. Soc. Mass Spectrom.* **2000**, *11*, 1036. (e) Ruan, C.; Rodgers, M. T. *J. Am. Chem. Soc.* **2004**, *126*, 14600. (f) Ryzhov, V.; Dunbar, R. C. *J. Am. Soc. Mass Spectrom.* **2000**, *11*, 1037. (g) Amicangelo, J. C.; Armentrout, P. B. *J. Phys. Chem. A* **2000**, *104*, 11420. (h) Wouters, J. *Protein Sci.* **1998**, *7*, 2472. (i) Armentrout, P. B.; Rodgers, M. T. *J. Phys. Chem. A* **2000**, *104*, 2238.
- (15) (a) Sponer, J. E.; Glahe, F.; Leszczynski, J.; Lippert, B.; Hobza, P.; Sponer, J. *J. Phys. Chem. B* **2001**, *105*, 12171. (b) Sponer, J.; Sabat, M.; Gorb, L.; Leszczynski, J.; Lippert, B.; Hobza, P. *J. Phys. Chem. B* **2000**, *104*, 7535. (c) Gresh, N.; Spackova, N.; Sponer, J. E.; Leszczynski, J.; Sponer, J. *J. Phys. Chem. B* **2003**, *107*, 8669. (d) Close, D. M.; Crespo-Hernández, C. E.; Gorb, L.; Leszczynski, J. *J. Phys. Chem. A* **2006**, *110*, 7485. (e) Pavelka, M.; Shukla, M. K.; Leszczynski, J.; Burda, J. V. *J. Phys. Chem. A* **2008**, *112*, 256. (f) Allen, R. N.; Shukla, M. K.; Burda, J. V.; Leszczynski, J. *J. Phys. Chem. A* **2006**, *110*, 6139. (g) Burda, J. V.; Sponer, J.; Leszczynski, J.; Hobza, P. *J. Phys. Chem. B* **1997**, *101*, 9670. (h) Sponer, J.; Sabat, M.; Burda, J. V.; Leszczynski, J.; Hobza, P. *J. Phys. Chem. B* **1999**, *103*, 2528. (i) Shukla, M. K.; Leszczynski, J. *J. Phys. Chem. B* **2008**, *112*, 5139.
- (16) (a) Rannulu, N. S.; Amunugama, R.; Yang, Z.; Rodgers, M. T. *J. Phys. Chem.* **2004**, *108*, 6835. (b) Yang, Z.; Rodgers, M. T. *Int. J. Mass Spectrom.* **2004**, *241*, 225.
- (17) Cwiklik, B. J.; Slavicek, P.; Cwiklik, L.; Nolting, D.; Winter, B.; Jungwirth, P. *J. Phys. Chem. A* **2008**, *112*, 3499.
- (18) Cwiklik, B. J.; Slavicek, P.; Nolting, D.; Winter, B.; Jungwirth, P. *J. Phys. Chem. B* **2008**, *112*, 7355.
- (19) McFail-Isom, L.; Xiuqi, S.; Williams, L. D. *Biochemistry* **1998**, *37*, 17105.
- (20) (a) Vijay, D.; Sastry, G. N. *Phys. Chem. Chem. Phys.* **2008**, *10*, 582. (b) Priyakumar, U. D.; Sastry, G. N. *Tet. Lett.* **2003**, *44*, 6043. (c) Priyakumar, U. D.; Punagai, M.; Krishnamohan, G. P.; Sastry, G. N. *Tetrahedron* **2004**, *60*, 3037.
- (21) (a) Vijay, D.; Zipse, H.; Sastry, G. N. *J. Phys. Chem. B* **2008**, *112*, 8863. (b) Reddy, A. S.; Vijay, D.; Sastry, G. M.; Sastry, G. N. *J. Phys. Chem. B* **2006**, *110*, 2479. (c) Reddy, A. S.; Vijay, D.; Sastry, G. M.; Sastry, G. N. *J. Phys. Chem. B* **2006**, *110*, 10206. (d) Vijay, D.; Sastry, G. N. *Chem. Phys. Lett.* **2010**, *485*, 235.
- (22) Boys, S. F.; Bernardi, R. *Mol. Phys.* **1979**, *19*, 553.
- (23) Bader, R. F. W. *Atoms in Molecules. A Quantum Theory*; Clarendon: Oxford, U.K., 1990.
- (24) Frisch, M. J.; Trucks, G. W.; Schlegel, H. B.; Scuseria, G. E.; Robb, M. A.; Cheeseman, J. R.; Montgomery, J. A., Jr.; Vreven, T.; Kudin, K. N.; Burant, J. C.; Millam, J. M.; Iyengar, S. S.; Tomasi, J.; Barone, V.; Mennucci, B.; Cossi, M.; Scalmani, G.; Rega, N.; Petersson, G. A.; Nakatsuji, H.; Hada, M.; Ehara, M.; Toyota, K.; Fukuda, R.; Hasegawa, J.; Ishida, M.; Nakajima, T.; Honda, Y.; Kitao, O.; Nakai, H.;

Klene, M.; Li, X.; Knox, J. E.; Hratchian, H. P.; Cross, J. B.; Adamo, C.; Jaramillo, J.; Gomperts, R.; Stratmann, R. E.; Yazyev, O.; Austin, A. J.; Cammi, R.; Pomelli, C.; Ochterski, J. W.; Ayala, P. Y.; Morokuma, K.; Voth, G. A.; Salvador, P.; Dannenberg, J. J.; Zakrzewski, V. G.; Dapprich, S.; Daniels, A. D.; Strain, M. C.; Farkas, O.; Malick, D. K.; Rabuck, A. D.; Raghavachari, K.; Foresman, J. B.; Ortiz, J. V.; Cui, Q.; Baboul, A. G.; Clifford, S.; Cioslowski, J.; Stefanov, B. B.; Liu, G.; Liashenko, A.; Piskorz, P.; Komaromi, I.; Martin, R. L.; Fox, D. J.; Keith, T.; Al-Laham, M. A.; Peng, C. Y.; Nanayakkara, A.; Challacombe, M.; Gill, P. M. W.; Johnson, B.; Chen, W.; Wong, M. W.; Gonzalez, C.; Pople, J. A. *Gaussian 03, Revision C.1*; Gaussian, Inc.: Pittsburgh, PA, 2003.

(25) (a) Dang, L. X.; Feller, D. *J. Phys. Chem. B* **2000**, *104*, 4403. (b) Fredericks, S. Y.; Jordan, K. D.; Zwier, T. S. *J. Phys. Chem.* **1996**, *100*, 7810. (c) Rao, J. S.; Dinadayalane, T. C.; Leszczynski, J.; Sastry, G. N. *J. Phys. Chem. A* **2008**, *112*, 12944.

(26) Scott, P. C.; Radom, L. *J. Phys. Chem.* **1996**, *100*, 16502.

(27) (a) Perchard, C.; Bellocq, A. M.; Novale, A. *J. Chem. Phys.* **1965**, *62*, 1344. (b) King, S. T. *J. Phys. Chem.* **1970**, *74*, 2133.

(28) Barman, A.; Taves, W.; Prabhakar, R. *J. Comput. Chem.* **2009**, *30*, 1405.

(29) Marincola, F. C.; Casu, M.; Saba, G.; Manetti, C.; Lai, A. *Phys. Chem. Chem. Phys.* **2000**, *2*, 2425.

(30) (a) Bindu, P. H.; Sastry, G. M.; Sastry, G. N. *Biophys. Res. Commun.* **2004**, *320*, 461. (b) Chourasia, M.; Sastry, G. M.; Sastry, G. N. *Biophys. Res. Commun.* **2005**, *3336*, 961.

(31) Thoden, J. B.; Miran, S. G.; Phillips, J. C.; Howard, A. J.; Raushel, F. M.; Holden, H. M. *Biochemistry* **1998**, *37*, 8825.

(32) (a) D'Alessandro, M.; Aschi, M.; Paci, M.; Nola, A. D.; Amadei, A. *J. Phys. Chem. B* **2004**, *108*, 16255. (b) Pelmenschikov, V.; Siegbahn, E. M. *Inorg. Chem.* **2005**, *44*, 3311.

(33) (a) Genis, C.; Sippel, K. H.; Case, N.; Cao, W.; Avvaru, B. S.; Tartaglia, L. J.; Govindasamy, L.; Tu, C.; McKenna, M. A.; Silverman, D. N.; Rosser, C. J.; McKenna, R. *Biochemistry* **2009**, *48*, 1322. (b) Valee, B. L.; Auld, D. S. *Proc. Natl. Acad. Sci. U.S.A.* **1990**, *87*, 220.

(34) Dudev, T.; Lim, C. *Annu. Rev. Biophys.* **2008**, *37*, 97.